# Interaction of electrically evoked responses in networks of dissociated cortical neurons

Pieter Laurens Baljon,[1,*] Michela Chiappalone,[2] and Sergio Martinoia[1,2]
[1]*Department of Biophysical and Electronic Engineering, Neuroengineering and Bio-Nano Technology Group, University of Genova, Via Opera Pia 11a, 16145 Genova, Italy*
[2]*Department of Neuroscience and Brain Technologies, Italian Institute of Technology, Via Morego 30, 16163 Genova, Italy*
(Received 13 May 2009; revised manuscript received 20 July 2009; published 18 September 2009)

In this work we describe the interaction of the responses of neuronal networks to pairs of electrical stimuli. For this we use networks of dissociated cortical neurons cultured on planar microelectrode arrays. We compare the response to pairs of stimuli with the response to a stimulus in isolation. To evaluate the influence of both stimuli we introduce a normalization of the root-mean square of the response. Furthermore we consider the response to a pair of stimuli as the linear superposition of the two constituents. The two methods combined show that the neuronal network strongly suppresses the second stimulus. At the same time we find a possible window of integration in which two stimuli from separate locations in the network can interact to form a new response.

DOI: 10.1103/PhysRevE.80.031906 PACS number(s): 87.80.−y, 87.85.−d

## I. INTRODUCTION

Understanding how neuronal networks process information requires investigations related to the transformation of complex inputs into firing patterns. One possible way to study input-output (I/O) functions is to use electrical pulses capable to induce correlated spiking activity in the target neurons. With control over the activity of a single neuron or of a neuronal population, we can probe activity-dependent mechanisms such as adaptation [1], synaptic plasticity [2], and even learning [3]. The design of the stimulus pattern is founded both on the hypothesized inner workings of that activity-dependent mechanism, and on an assumed transformation of electrical stimuli into spike trains. For intracellular stimulation this transformation is quite well understood [4,5] while for extracellular stimulation this is much less the case [6,7]. Here we focus on extracellular stimulation of dense networks of dissociated rat-cortical neurons [8]. The neurons are cultured on top of a grid of 60 microelectrodes (microelectrode arrays: MEA) that provide a bidirectional interface with the network. This setup is used extensively to study network dynamics (firing and bursting patterns) and to investigate activity-dependent mechanisms at the network level [9–14]. The use of such in-vitro cultures permits to investigate basic mechanisms that are independent of specific brain regions and allows focusing on the understanding of changes induced by the stimulation at the network level. However, to study how the evoked activity brings about these global changes, it is essential to understand what activity the stimuli evoke. Extracellular stimulation evokes a more complex response than intracellular stimulation because multiple elements are activated simultaneously [6,7,15]. This complexity is further aggravated in large-scale networks (as for networks of dissociated neurons or organotypic cultures) by their complex dynamics and typical bursting behavior: in these networks an electrical stimulus often evokes a burst of activity containing tens of spikes on most of the active electrodes over a period of several hundreds of milliseconds [15,16]. As a result, in complex stimulation protocols, responses to individual stimuli inevitably overlap and interact. These interactions are hard to predict due to the limited knowledge of the connections in the network and of the geometry of the space surrounding the electrode and due to the unavoidable undersampling of the network elements.

A considerable amount of literature exists on the network activity during complex stimulation protocols. A large part of this work regards the steady-state condition during stimulation [17–19]. In I/O terms, the current work focuses on the transient response of the network by considering only pairs of stimuli. The work by Eytan *et al.* [20] investigates the interaction between rare (at low-frequency) and frequent stimuli. The authors show that the presence of frequent stimuli amplifies the response to rare stimuli that are tens of seconds apart. By contrast, the results presented here describe immediate interactions between responses on a time scale of 10 ms to a second. The interaction of responses on a subsecond time scale has been partly exploited to design a neural code to control a robot [21] and to reduce variability in the network response [22]. However, these studies did not quantify those interactions as such, but rather focused on the behavioral performances of the robot.

In this work we specifically investigate how the evoked responses of two stimuli are combined: what is the effect of a stimulus A on the response evoked by another stimulus B? We answer this question both for stimuli A and B applied from the same electrode, and from two separate electrodes. Such an effect would clearly depend on the delay between the two stimuli. When the two stimuli are sufficiently distant in time, the individual responses can be considered independent. Thus, we test the two null hypotheses that the response to the pair is governed completely by either one of the stimuli constituting the pair. Any significant deviation illustrates the interaction of the two stimuli. Furthermore, we discuss a method to estimate the relative contribution of each of the two stimuli in the pair.

*Corresponding author; pieter.laurens@unige.it

 

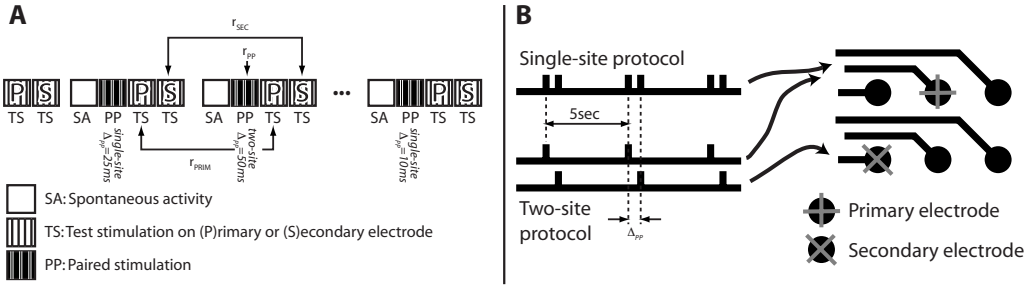


FIG. 1. Experimental design. (A) The time line of the different phases in the experiment. The test response on the primary and secondary electrode (vertical black lines) is recorded before and after each paired-stimulation (double white lines) recording. The vertically printed labels under the paired-stimulation phases give a possible, random ordering for this experiment. The sequence, i.e., spontaneous activity, paired stimulation and test stimulation, is repeated eight times; here only three are shown. The labels on the arrows illustrate for one particular phase of paired stimulation (two-site stimulation, $\Delta_{PP}=50$ ms) from which phases the firing rate profiles $r(t)$ are computed that are used for the comparisons (see text). (B) Illustration of the difference between the single- and two-site protocols. Whereas in the single-site protocol both pulses are applied form the same electrode (+), in the two-site protocol pulses are applied from the two separate electrodes (first + then $x$).

## II. METHODS

### A. Cell cultures

Animal care and all experimental procedures were carried out in accordance with the European Communities Council Directive of 24 November 1986 (86/609/EEC). Timed-pregnant Sprague-Dawley rats were sacrificed after which embryos at embryonic day 18 were extracted by caesarean section. Inner-brain structures were removed and the cortical area was dissociated by mechanical trituration following treatment with 0.125% trypsin solution. The cortical cells were then plated onto microelectrode arrays (MEAs, Multichannel systems, Reutlingen, Germany) at a final density of around 2000 cells/mm$^2$. MEAs had been precoated with Laminin and Poly-D-Lysine to promote adhesion of the neurons. The cells were kept in an incubator at 5%$CO_2$ and 95%$O_2$ and 100% relative humidity at 37 °C in B27-supplemented Neurobasal medium [23]. The medium was changed once a week. All experiments were performed between DIV20 and DIV34. At this age the network is considered in a stable and mature stage in which connectivity is established and in which small fluctuating bursting behavior is observed [24,25]. For the experiments presented here, we used 13 cultures from two batches.

### B. Recording of electrophysiological signals

The MEAs contained 60 TiN electrodes with a diameter of 30 $\mu$m and an interelectrode distance of 200 $\mu$m. The neurons adhere to the substrate of the MEAs covering all electrodes. The voltage on the electrodes relative to a large bath Ag/AgCl reference electrode was bandpass filtered between 10 Hz and 3 kHz and sampled at 10 kHz using the MEA1060BC filter amplifier (Multichannel systems, Reutlingen, Germany) to be stored on a hard drive for offline analysis. If the neuron has sufficient electrochemical coupling with the electrode surface, individual action potentials can be discerned in the recorded signal [26]. These action potentials were detected using an algorithm applying a threshold at eight times the standard deviation of the background noise [27]. All cultures had 50–60 active channels. The action potentials can originate from multiple neurons and could in theory be separated using spike sorting techniques [28]. Since our analyses are not strictly related to individual neurons and the collective activity patterns are known to influence spike forms we decided to not use spike sorting.

### C. Experimental protocols

All analyses presented below describe activity evoked by electrical stimulation. Stimuli were applied as positive-then-negative voltage-controlled pulses and were generated by a commercial stimulator (STG1008, Multichannel systems, Reutlingen, Germany). The amplitude was 1.5–2.0 V peak-to-peak relative to a large Ag/AgCl reference electrode in the bath and was kept fixed for an entire experiment. The duration of a pulse was 400 $\mu$s (200 $\mu$s for both the positive and negative part). After a stimulus the blanking circuit in the amplifier kept the electrodes disconnected for an additional 400 $\mu$s to reduce the stimulation artifact. To avoid any possible interference we discarded the spikes detected in the 2 ms after a stimulus.

The goal of the experiments was to describe the effect of one pulse on the activity evoked by another pulse. Therefore we stimulated the culture with pairs of stimuli and compared the activity evoked by the pair with that evoked by single stimuli. The phases are indicated as "paired stimulation" and "test stimulation," respectively. A phase of "test stimuli" consisted of 30 stimuli applied to an electrode at 0.2 Hz. The design of the experiment is illustrated in Fig. 1(A). Before each experiment we recorded phases of test stimulation from 5–6 electrodes and from those we selected the two electrodes that evoked the most reproducible and network-wide response for paired stimulation [11]. Then we applied the eight (see below) paired-stimulation protocols. Between each phase of paired stimulation we recorded a phase of test stimulation on the two electrodes selected for paired stimulation and an additional 2 min of spontaneous activity.

In the paired-stimulation phases we applied 60 pairs of stimuli to the network at a frequency of 0.2 Hz (i.e., the

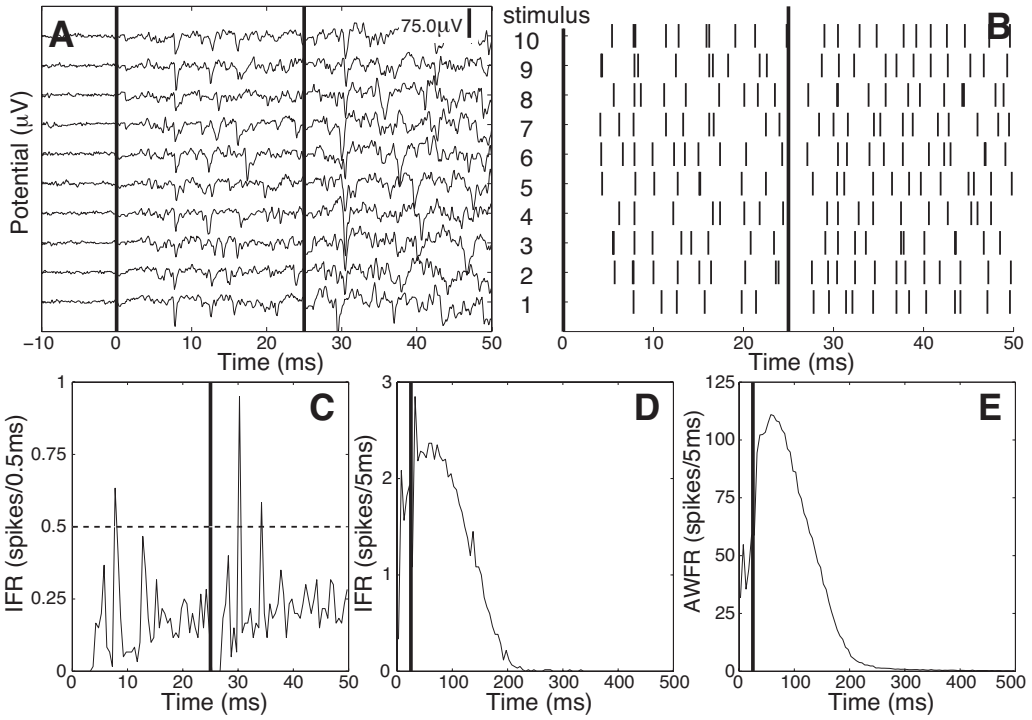


FIG. 2. Chronological ordering of the analyses of evoked activity from a two-site stimulation phase with $\Delta_{PP}=25$ ms. The thick vertical lines indicate the arrival of the two stimuli. Data in panels A–D are from one representative electrode. (A) The raw recordings following the first 10 (of 60) pairs from $t=-10\ldots50$ ms relative to the first stimuli. This type of figure is of great help in assuring the proper functioning of stimulator, amplifier and peak detection algorithms. (B) The same data as in A after peak detection to visualize the functional effect of stimulation and reproducibility of the response. (C)–(E) The PSTH is a histogram of delays of spikes after a stimulus and can be transformed into an estimate of the instantaneous firing rate (IFR). The PSTHs are estimated from all 60 responses with a bin size of (C) 0.5 ms and [(D) and (E)] 5 ms. In panel C the dashed line indicates the threshold for detecting direct action potentials (see text). The population PSTH in panel E is obtained by pooling spikes from all electrodes to get an estimate of the array-wide firing rate (AWFR). Firing rates are referred to as $r(t)$ in the text with labels in sub- and superscript and $t$ relative to the stimulus as in these graphs.

delay between the two first stimuli of subsequent pairs was 5 s). For the interval between pulses (Interpulse interval, denoted $\Delta_{PP}$) we used values of 10, 25, 50, and 100 ms in "short-$\Delta_{PP}$ experiments" and 100, 250, 500, and 1000 ms in a second series of "long-$\Delta_{PP}$ experiments." The first pulse was applied from the so-called primary electrode. In the "single-site" protocol the second pulse was applied from the same primary electrode. In the "two-site" protocol the second pulse was applied from a different electrode: the secondary electrode [see Fig. 1(B)]. The short-$\Delta_{PP}$ experiments were performed on eight cultures. Subsequently we performed long-$\Delta_{PP}$ experiments on five cultures to understand the recovery of the responsiveness. These cultures are highly connected and activity does not necessarily spread over the network like a wave. It has been shown that electrical stimulation directly (i.e., nonsynaptically) activates neuronal elements far away with only slightly lower probability than those close by [8]. Therefore, the selection of the two stimulating electrodes was not based on their relative spatial location as we expect the effect of distance to be very small. We limited our consideration of a spatial effect to the two pulses either being delivered from the same (single-site protocol), or separate electrodes (two-site protocol).

For each network we recorded eight phases of paired-pulse stimulation in random order: four different values for $\Delta_{PP}$ in both the single-site and two-site protocol. An entire protocol took roughly 150 min in which the culture was continuously stimulated except for the 2 min recordings of spontaneous activity.

### D. Data analysis

To describe the evoked activity we use the poststimulus time histogram (PSTH). The PSTH is the histogram of the latencies of spikes after a stimulus. We construct the histogram using spikes with a latency up to 500 ms and we use a bin size of 5 ms. This bin size is a compromise between a smooth graph and sufficient temporal detail. Figure 2(D) is an example of a PSTH where the other panels illustrate the intermediate steps in its calculation from the raw signal. The PSTH can be transformed into an estimate of the instantaneous firing rate $r(t)$ at time $t$ relative to a stimulus by dividing the counted values by the number of stimuli and the bin width. We introduce $r_{PP}(t)$ as the instantaneous firing rate relative to the first of a pair of stimuli. $r_{PRIM}^{PRE}(t)$ and $r_{PRIM}^{POST}(t)$ designate the estimated firing rate after stimulating the primary electrode before and after the paired stimulation, respectively. When pooling the test stimuli before and after the paired stimulation we indicate the firing rate $r_{PRIM}(t)$. The firing rate after stimulating the secondary electrode is indicated as $r_{SEC}(t)$. Figure 1(A) shows from which phases the respective $r(t)$ are obtained. We can construct these PSTHs

based on the activity at a single channel or after pooling spikes from all electrodes. The latter produces the population PSTH [PPSTH; see Fig. 2(E)] [29].

In the period immediately following a stimulus, i.e., in the first 20 ms, we often see spikes that are evoked with high reliability and temporal precision [15], dubbed direct responses [8] or direct action potentials (dAPs) [30]. This behavior is distinct from the later phase where the exact timing of individual spikes seems indeterminate, even though the average over multiple responses is very stable. We will analyze the early and late response separately. For the late response we use a window of 20…350 ms after the stimulus. For the early response we use a thresholding algorithm to extract the dAPs in the first 20 ms (see below).

### E. Quantifying changes in the evoked activity

In all cases the pair response $r_{PP}(t)$ is compared to the test response on the two electrodes constituting the pair: $r_{PRIM}(t)$ and $r_{SEC}(t)$. We evaluate the difference between responses with a normalization of the root-mean square (rms) value. We also discuss a method to decompose the pair response into the contributions of the two pulses as a linear combination.

Of any spike observed after the second pulse it is impossible to determine whether the first or second pulse in the pair has evoked it or whether it is spontaneous. With the rms we can only test the hypothesis of there being no effect of one of the pulses. There are two hypotheses we can test with these data:

-$H_1$: the second pulse has no effect on the activity evoked by the pair as a whole.

-$H_2$: the first pulse has no effect on the activity evoked by the pair as a whole.

The hypotheses imply two different comparisons between pair and test response. In Fig. 3 these comparisons are illustrated. For both hypotheses the same part of the pair response is used, represented by the gray area in panel 3C. $\Delta_{PP}$ indicates the interval between pulses in the pair, i.e., the interpulse interval. We use the window $w_{pair}=\{t|\Delta_{PP}+20<t<\Delta_{PP}+350\ \text{ms}\}$ relative to the first stimulus in the pair—as in the definition of $r_{PP}(t)$. Note that this window is equivalent to $\{t|20<t<350\ \text{ms}\}$ relative to the second stimulus. Under $H_1$, the pair response is compared to window $w_{test}^{H1}=\{t|\Delta_{PP}+20<t<\Delta_{PP}+350\ \text{ms}\}$ in $r_{PRIM}(t)$ (gray area in panel A). Under $H_2$ the pair response is compared to the window $w_{test}^{H2}=\{t|20<t<350\ \text{ms}\}$ in $r_{SEC}(t)$ for the two-site protocol (gray area in panel B) or in $r_{PRIM}(t)$ for the single-site protocol.

### F. Normalized root-mean square

We describe the difference between two time courses with the root mean square of the difference between $r_{PP}(t)$ and the relevant $r_k(t)$ as described above with $k$ either PRIM or SEC. If the test response $r_k(t)$ is obtained by averaging $r_k^{PRE}(t)$ and $r_k^{POST}(t)$ we define the difference between the pair and test response under null hypothesis $h$ as

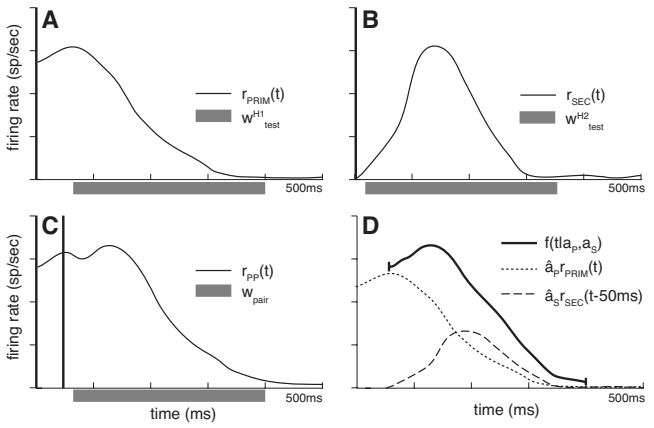


FIG. 3. Illustration of how responses from two separate electrodes might be combined for fictitious data from a two-site protocol with $\Delta_{pp}=50$ ms. Panels A and B show the response at an electrode after stimulating in isolation the primary (a) and secondary (b) electrode, respectively. This is referred to as "test stimulation." Panel C shows the response when the two electrodes are stimulated in close succession (paired stimulation). The gray bars below the horizontal axes depict the windows used for comparisons with the normalized rms (see text). Panel D illustrates the fitting method. The observed pair response in panel C is reconstructed as a linear combination of the test responses in panels A and B (see text).

$$D_h(r_{PP},r_k)=\frac{\Psi[r_{PP}(w_{pair})-r_k(w_{test}^h)]}{\Psi[r_k^{PRE}(w_{test}^h)-r_k^{POST}(w_{test}^h)]}\frac{\sqrt{60}}{\sqrt{30}} \quad (1)$$

with the standard definition for root-mean square,

$$\Psi[r(t)]=\sqrt{\frac{1}{T}\sum_{t=1}^{T}r(t)^2}. \quad (2)$$

The test response from electrode $k$ is estimated from two samples of 30 stimuli. We use the rms value of the difference between $r_k^{PRE}$ and $r_k^{POST}$ as a measure of intrinsic variability. We use the intrinsic variability to normalize the difference between test and pair response. The factor $\sqrt{2}$ in Eq. (1) corrects for the different number of stimuli used to estimate the firing rates in the nominator and denominator and the resultant difference in expected variability. Under the null hypothesis $h$ the expected value for $D_h$ is 1.0 and the parameter can be interpreted as multiples of intrinsic variability of the response.

### G. Pair response as a linear combination of test stimuli in isolation

With the normalized rms we can only test whether something changes, while it remains difficult to assess exactly what has changed. In a method we reconstruct the observed pair response [Fig. 3(C)] from the two test responses constituting the pair (Fig. 3, panels A and B). In short, with $\Delta_{PP}$ the interpulse interval, we make a linear combination of the two functions $r_{PRIM}(t)$ and $r_{SEC}(t-\Delta_{PP})$, that best matches the observed pair response $r_{PP}(t)$ [Fig. 3(D)]. A big advantage of this approach is that it does not require the assumption that

one of the responses is unaffected by the other stimulus.

The linear combinations of the test responses are expressed as

$$f(t|a_p,a_s) = a_p r_{PRIM}(t) + a_s r_{PRIM}(t\text{-}\Delta_{PP}), \quad (3)$$

$$f(t|a_p,a_s) = a_p r_{PRIM}(t) + a_s r_{SEC}(t\text{-}\Delta_{PP}) \quad (4)$$

for the single- and two-site protocol, respectively. In reality the $a_{\cdot}$ is fitted as their square to allow only positive values. We then minimize the difference between the observed pair response $r_{PP}(t)$ and Eq. (1) or (2) over the window $w_{fit} = \{t \,|\, \Delta_{PP} < t < \Delta_{PP} + 350 \text{ ms}\}$. The difference can be expressed by the chi-square value,

$$\chi^2(a_p,a_s) = \sum_{t \in w_{fit}} \{[f(t|a_p,a_s) - r_{PP}(t)]^2/\sigma(t)\} \quad (5)$$

with

$$\sigma(t) = \sqrt{r_{PP}(t)}. \quad (6)$$

Equation (6) reflects the notion that uncertainty is generally higher for higher values of the parameter. The qualitative outcome of the fitting is robust to the exact form of the variance. Now, the minimization procedure can be formalized as

$$\arg\min_{a_p,a_s} \chi^2(a_p,a_s). \quad (7)$$

Equation (7) is solved by the Levenberg-Marquardt algorithm [31] in MATLAB (The Mathworks Inc., Natick, MA). To ensure the proper functioning of the fitting algorithm we smooth the PSTH with a rectangular window of 25 ms and exclude electrodes that contain less than 10 bins larger than zero (out of 70 bins $\times$ 5 ms = 350 ms). Furthermore $r_{PRIM}$, $r_{SEC}$, and $r_{PP}$ are all normalized to an area of 1.0. From this fit we extract several relevant parameters,

(1) The two scaling parameters that best fit the paired response as a sum of the two test responses.

(2) The fraction of electrodes where fixing one scaling parameter actually improves the goodness of fit.

For the goodness of fit we use the reduced chi-square statistic to correct the error between model and observations for the number of parameters $p$ in the model. This statistic is computed $\varepsilon = X^2/(N-p-1)$ with $N$ the number of observations, i.e., the number of nonzero bins in the PSTH out of the total 70. Because $p=2$ with both $a_p$ and $a_s$ free but $p=1$ when we keep one parameter fixed at 1.0, a small increase in $X^2$ by fixing the parameter might be offset by the reduced denominator and thus improve the goodness of fit.

The parameters $a_p$ and $a_s$ can be interpreted in two ways. They either represent the probability of observing the pattern as a whole for any individual stimulation, and averaging over stimuli would give a linear combination. Alternatively they represent the presence of that pattern in a mixture of both individual responses.

### H. Detection and analysis of direct action potentials

We detect changes in the direct action potentials using a PSTH with 0.5 ms bin size in the first 20 ms after stimulation. Bins that exceed 0.50 spikes per stimulus both before and after paired stimulation are classified as a dAP. It is highly unlikely that a bin exceeds 0.50 in both phases by chance as it corresponds to an instantaneous firing rate of 1000 Hz [see Fig. 2(C)]. We combine adjacent bins surpassing the threshold, and extend the dAP by 0.5 ms on both sides to obtain a window relative to the stimulus. We estimate the baseline peak height by pooling responses before and after the paired stimulation. We then take the ratio of the peak height after the second pulse in the pair and the baseline peak height. This is called the ratio of reliability as the peak height is an estimate for how reliably the action potential is evoked.

### I. Statistical analysis

We summarize results for normalized rms ($D_{H1}$ and $D_{H2}$) and fitting ($a_p$ and $a_s$) from individual electrodes by taking the median value over the active channels. Active channels are those that on average respond with at least five spikes per stimulus. We exclude the primary and secondary stimulating electrode. The ratios of reliability are combined by taking the median over all dAPs in a network rather than over electrodes. We investigate the difference between conditions by comparing the mean over the individual experiments. In the graphs we draw error bars representing the standard deviation among experiments. We test for an effect of stimulation protocol (single-site or two-site) on the parameter for change with a paired $t$-test for all experiments and values of $\Delta_{PP}$ that were recorded for both protocols. In the rest of the text, results are summarized as one-sided 95% confidence intervals for the mean normalized rms. Suppression is evaluated by the upper bound of the 90% confidence interval, whereas integration is evaluated by the lower bound of the 90% confidence interval.

The continuous stimulation for 2 h, albeit at a low frequency, requires us to ascertain the stability of the evoked activity. For this we use the PPSTH. We exclude all phases of paired stimulation following a phase of test stimulation in which the Pearson correlation coefficient $r$ between the PPSTH of that phase and that of the initial test-stimulus phase is smaller than 0.8. In principle the methods are resilient against changes in the network dynamics since the pair response is compared to the two adjacent test responses. However, changes (usually decreases) in the PPSTH shape pointed to an overall depression of the culture's activity and therefore we decided to discard those unstable phases (23 out of 112 phases). Furthermore, eight data were analyzed separately because their small denominator in Eq. (1) gave them a too big influence on the normalized rms. The fitting procedure was able to provide a good explanation for these particular situations. Therefore, these data (i.e., outliers) are indicated as single points in the figures and separately described and discussed in the results section.

## III. RESULTS

The dynamics of the evoked responses show remarkably stable patterns, in nature similar to the spontaneously occur-

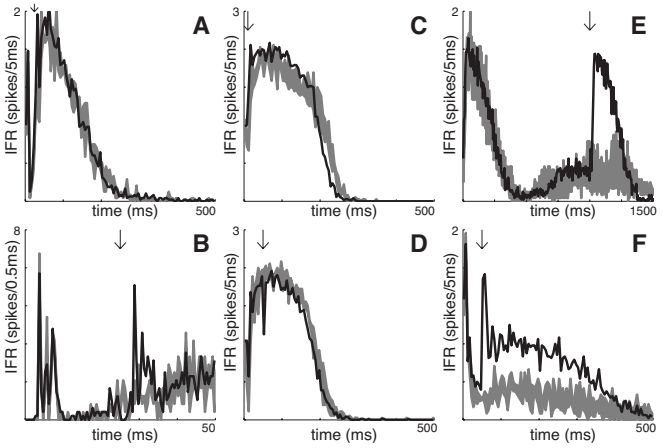


FIG. 4. Examples of changes of the response when applying paired pulses. The gray area indicates the range of values observed for the test responses before and after the pair response. The lower bound at time $t$ is the smaller one of $r^{\mathrm{PRE}}_{\mathrm{PRIM}}(t)$ and $r^{\mathrm{POST}}_{\mathrm{PRIM}}(t)$ while the upper bound is the larger one. The pair response itself is represented by the black trace. Under $H_1$ we expect that the black trace and the gray area overlap. Arrows indicate the arrival of the second stimulus. All data are from single electrodes (cf. panels 2C and 2D). (A) A typical pair response composed solely of the primary response in the single-site protocol at $\Delta_{\mathrm{PP}}=25$ ms. (B) The same response at higher time resolution; only the first 50 ms. The early response is clearly visible and is evoked by the second pulse in the pair as well. [(C) and (D)] Two responses to two-site stimulation from the same electrode and network at two different values for $\Delta_{\mathrm{PP}}$. C: 10 ms and D: 50 ms. The trace in panel C is more different from the test response than is D. (E) After 1000 ms the network is again able to evoke activity. (F) A typical response from a rejected network where the response has become much elongated spanning 500 ms.

ring bursts described in previous work [24,25]. This is illustrated by panels A–E in Fig. 4 that contains examples of test and pair responses for different stimulation regimes. The gray band represents the variability between the two test responses obtained before and after the paired stimulation and the black line represents the paired response. Panel 4F shows one of the rejected phases with the much elongated response.

Studying the interaction of responses elicited by the proposed protocols of paired-pulse stimulation, we found out, as main result, that the response to a subsequent stimulus is much suppressed if that stimulus falls inside a specific window after the first pulse both for single-site and two-site stimulation. In the following paragraphs we illustrate the obtained experimental results together with the obtained fitting procedures to quantify the interaction of the evoked responses at network level. In all the figures data are presented as mean with standard deviation to illustrate the spread among experiments.

### A. Single-site protocol

Figure 5(A) shows that for two stimuli from the same electrode and an interval up to 250 ms the rms coincides well with the value under $H_1$. This means that the expected difference between the primary test response and pair response is similar to the difference between two subsequent samples of primary test responses of the same size. Moreover, the upper bound of the confidence intervals ranges from 1.42 to 1.75. Thus for each interpulse interval $\Delta_{\mathrm{PP}}$, in 95% of the cases the difference between pair and primary test response will be less than 1.75 times the difference between two samples of primary test responses. The much larger absolute values and variability between experiments makes it safe to reject $H_2$, i.e., that the second stimulus should govern the pair response for all the values of $\Delta_{\mathrm{PP}}$ except the shortest

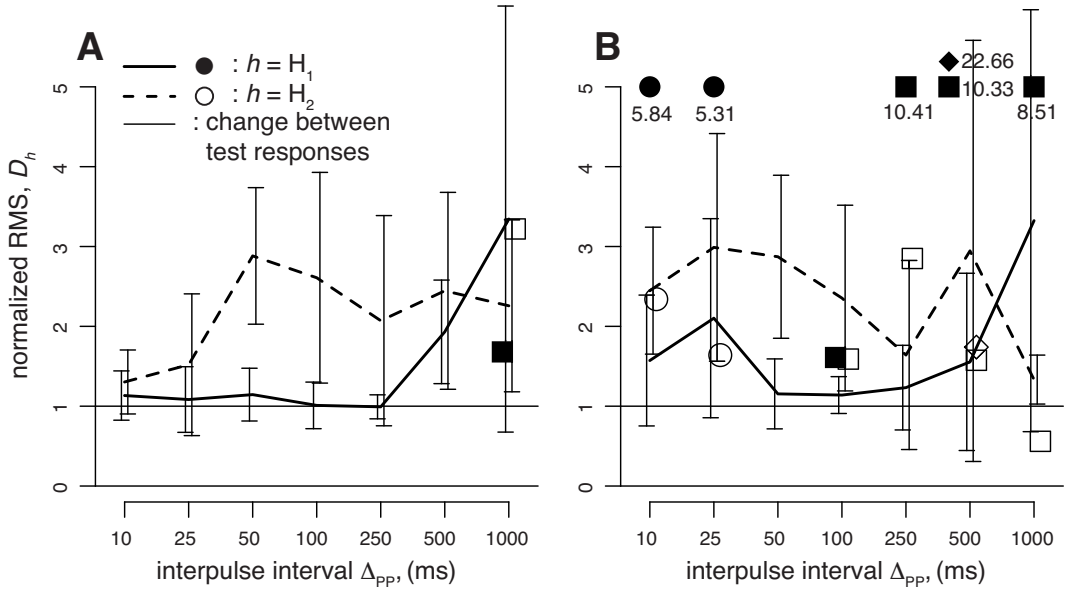


FIG. 5. The normalized rms expresses the difference between the pair and test response as a multiple of the difference between the response from two subsequent phases of test stimuli. Panel A shows the results for the single-site protocol and (B) for the two-site protocol. The symbols represent outliers, mainly due to a small denominator for normalization. These are analyzed separately.

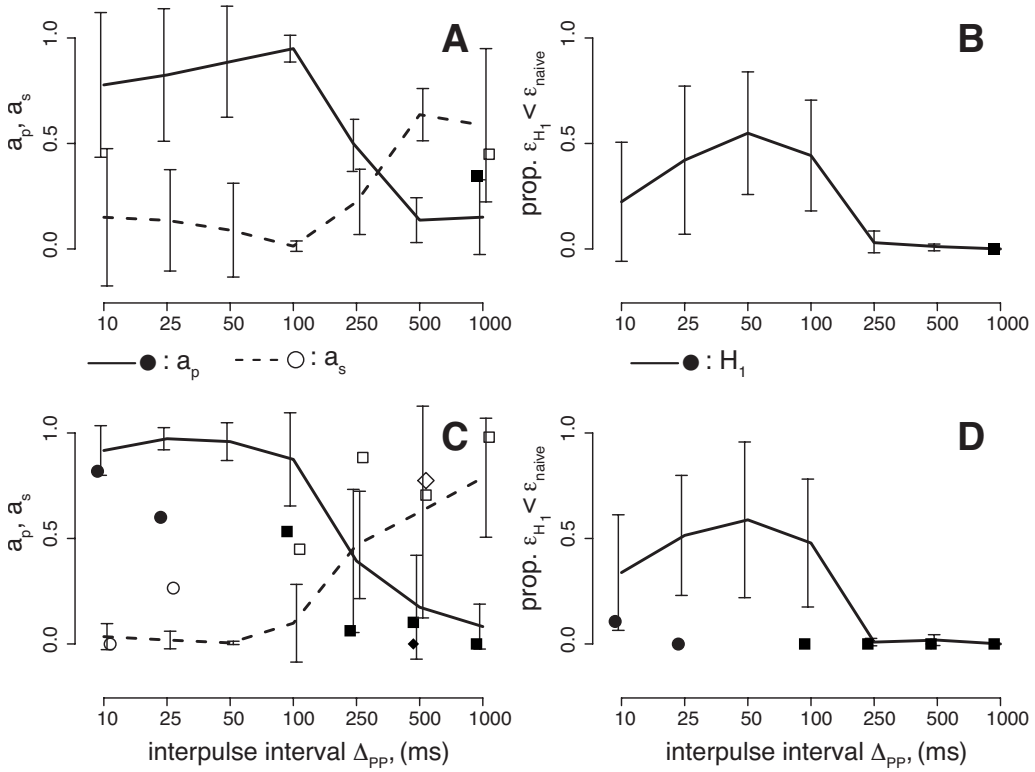


FIG. 6. Quantitative analysis of the pair response composition. The two rows show the results for the single-site (panels A and B) and two-site (panels C and D) protocol, respectively. The leftmost panels show the values for $a_p$ (solid) and $a_s$ (dashed) representing the contribution of the first ($a_p$) and second ($a_s$) stimulus. The rightmost panels give the proportion of electrodes in which the reduced chi-square statistic indicated as $\varepsilon$ for the naïve fit is larger than the reduced chi-square statistic under $H_1$, i.e., assuming $a_p$ is 1.0.

interval. For $\Delta_{PP}=10$ ms we expect that the low rms under $H_2$ is due to the similarity of the hypotheses: the two responses are shifted by only 2 bins. For $\Delta_{PP}=500$ and 1000 ms it is unlikely that the first stimulus governs the pair response, but the large variability and limited number of data make it impossible to quantify this.

### B. Two-site protocol

Considering all networks and interpulse intervals together, there is no structural difference in effect between the single- and two-site protocols. A paired *t*-test for a structural difference between conditions under $H_1$ including all networks and intervals is not significant for the normalized rms. This can be seen comparing panels A and B in Fig. 5 where the solid line in both panels shows a similar trend.

When we look at individual values for $\Delta_{PP}$ we do see interesting differences. For two stimuli from separate electrodes and a short interval, the lower bound of the one-sided 95% confidence interval for the normalized rms is 1.00 and 1.43 for $\Delta_{PP}=10$ and 25 ms, respectively. This means that the difference between test and pair response is at least as large as the difference between two samples of test responses, and on average 1.5 to 2 times larger. This is an interesting starting point for a possible "window of integration" in these networks. For the intermediate intervals 50, 100, and 250 ms the upper bound for the rms is 1.77, 1.71, and 1.98, respectively, while the means are 1.15, 1.14, and 1.23. Though the influence of a stimulus from a secondary electrode is likely to be larger than that of one from the primary electrode—up to twice as large as intrinsic variability, the difference is expected to be only 14–23 % more than the difference between two samples of test stimuli. Figures 4(C) and 4(D) shows two responses for two-site stimulation for $\Delta_{PP}=10$ ms (panel C) and $\Delta_{PP}=50$ ms (panel D). The pair response in panel D coincides much better with the test response than in panel C.

For $\Delta_{PP}=1000$ ms, we see that $H_2$ has become favorable over $H_1$. The mean rms is still expected larger than 1.0: the mean is 1.3, but the standard deviation is limited. The confidence interval does not give much information due to the limited number of data ($n=3$). However, together with the outliers, the data clearly show that the responsiveness starts to recover after 1 s but the differences between networks are too large to make any quantifications.

### C. Fitting the individual test responses

To better describe the individual contributions of the two stimuli we fitted the linear combination of the two test responses to the pair response. The fitted parameters for the two protocols are shown in panels A and C of Fig. 6. Apart from very clear time dependence, the graphs also provide good insight into the nature of the outliers. These will be mentioned in more detail below.

The fitting outcomes show that for $\Delta_{PP}<100$ ms the second pulse is not present in the pair response, whereas at

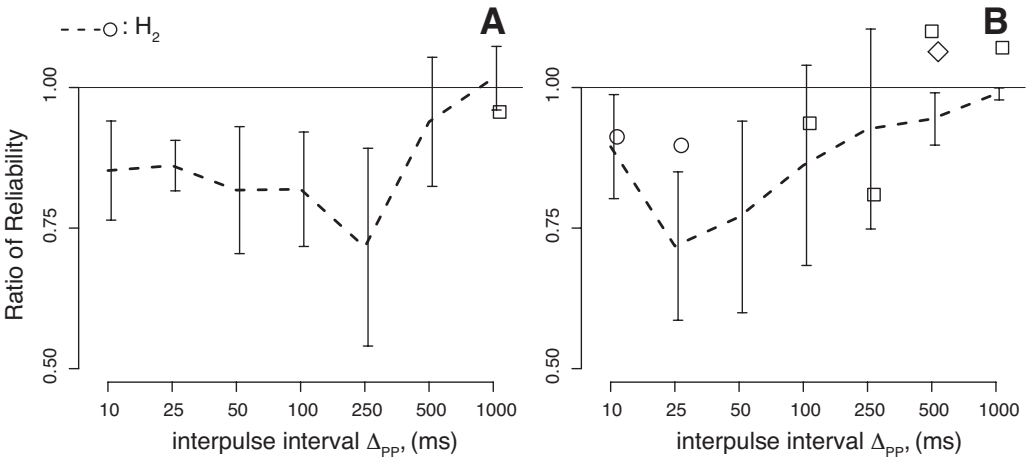


FIG. 7. Ratio of the dAP's reliability after the second stimulus in the pair and a stimulus in isolation. Panels A and B show the results for single- and two-site protocol, respectively. The traces show a very clear frequency effect, with the response returning to "normal" steadily when the interpulse interval exceeds the duration of the response. For the two-site protocol the effect shows slightly more spread but a very reliable return to baseline for $\Delta_{PP}=1000$ ms. Error bars indicate the standard deviation over the experiments.

1000 ms the form of the evoked response is almost completely determined by the second pulse. This supports that indeed the low rms for $H_2$ at short intervals for the single-site protocol are caused by the similarity of the hypotheses. The larger standard deviation for the two-site protocol at $\Delta_{PP}=100$ and 250 ms indicates that there is more variability among networks or that the combined response from two electrodes is not fitted as well by a linear combination. The evolution of the proportion of electrodes that actually see a decrease in reduced chi-square when adding the first response as a degree of freedom, supports the hypothesis that the primary response completely governs the form of the pair response up to $\Delta_{PP}=100$ ms [Figs. 6(B) and 6(D)]. A big advantage of this method is that it is able to explain points that for the normalized rms appeared as outliers. We can see whether the change is due to the (unexpected) presence of the secondary response [e.g., the circle at $\Delta_{PP}=25$ ms in the two-site protocol; Fig. 6(C)] or whether it is in fact not possible to reconstruct the response properly.

### D. Changes in the early response

The reliability of dAPs can be reduced by a preceding stimulus as illustrated in Fig. 7. If stimuli are applied from the same electrode, this ratio is significantly smaller than 1.0 ($p<.01$) for $\Delta_{PP}\leq 250$ ms. For the two-site protocol 25 ms $\leq\Delta_{PP}\leq 100$ ms the ratio is significantly ($p<.05$) smaller than 1.0. The lack of suppression in the two-site protocol for $\Delta_{PP}=10$ ms may be related to the integration of responses in this window as expressed by the rms being larger than 1.0. After 10 ms it is possible that the neurons at the secondary electrode have not received any synaptic input following the stimulation. Though for the two-site protocol the suppression effect is very variable between networks, for $\Delta_{PP}=1000$ ms there is no more effect of a preceding stimulus.

### E. Case reports of peculiar phases

The results described above are based on all networks that showed sufficient stability. Even though the trends described by the results are clear among these networks, some phases show remarkable deviances from these trends. These phases were left out of the statistical analyses and plotted separately in the figures. These phases originated from three networks indicated by a circle, square, and diamond shape. They were inspected carefully to gain insight into the origin of the suppression effect we observed for value of $\Delta_{PP}$ ranging from 50 to 250 ms. For the circle-coded experiments, the response to the primary electrode is only 3–6 spikes per channel compared to 20–50 in most other networks. For $\Delta_{PP}=100$ ms in the two-site condition, the square-coded network responds with 20–27 spikes per channel but here the secondary response is up to twice as large. Still, there are other networks with responses around 20 spikes that conform well to $H_1$ (data not shown). Other data on responses below 10 spikes are not available. It could be that it is a necessary but not sufficient condition for integration of inputs that the network fires below its maximum rate. This relates well to the suppression window for the two-site protocol coinciding with the typical AWFR profile of the response.

Furthermore, a small primary-response size may throw rms off course under $H_1$ when the interpulse interval exceeds the duration of evoked activity. Now any amount of activity evoked by the second stimulus is a large multiple of the inexistent activity assuming it is evoked by the first stimulus. An example of this is the two-site condition of the diamond- and square-coded networks for $\Delta_{PP}>100$ ms where rms is well beyond the scale of the figure. Here the fitting procedure indicates that the response is governed by the second stimulus with values well within the standard deviation over experiments. This effect is related to the metrics used rather than a network effect.

## IV. DISCUSSION AND CONCLUSIONS

In the previous section we gave an overview of the effects that govern the response of networks of dissociated cortical neurons to paired-pulse electrical stimulation. The main finding is that there is a time window of suppression of the

second response. This window is up to 250 ms long in which the response can be explained as were the response evoked by the first stimulus alone. By adding a series of experiments with longer delays between pulses we showed that the response to the second stimulus appears as a linear combination of the two single pulse responses and tends to dominate for large values of $\Delta_{PP}$ (500 ms and 1s delay). As might be expected, this recovery phenomenon shows large variability among networks.

The results furthermore point to an interesting difference depending on whether the two stimuli are applied from the same or separate electrodes. In the latter case there is a possibility for the second stimulus to alter the pair response if it falls within 50 ms of the first stimulus. Even if this effect is also subject to large variability among networks, it appears in many cases that in such a short window after the first stimulus (10–25 ms), a subsequent stimulus from a different electrode increases the network's overall response. What is relevant here is not the spatial distance between the two stimulating sites but the capability of the network to account for stimuli coming from distinct but interacting pathways. The observed change suggest that a kind of integration took place at the population level. This was also observed by Bakkum *et al.* [21] and would allow for selective integration of inputs that are temporally close. Another observation is that for two stimuli from distinct electrodes the maximum suppression coincides roughly with the time course of the burst after stimulation. The hypothesis that firing rate and suppression are related is supported by previous studies of excitability after a burst [18]. This hypothesis is also in line with the limited suppression both of the direct responses in the two-site protocol for $\Delta_{PP}=10$ ms [Fig. 7(B)] and of the late response in several of the networks with a small response to the first stimulus (circle- and square-coded experiments in Fig. 6). We plan to further investigate this hypothesis in future experiments.

As it has been shown in the literature, it is possible to induce lasting changes through repetitive low-frequency stimulation in both the spontaneous [32] and evoked activity [10,33]. Jimbo and colleagues used a train of high-frequency stimuli [9] on a single electrode inspired by intracellular studies. This work showed that changes are stimulation site, or pathway specific, rather than recording site specific. Similarly, polysynaptic interactions and association of pathways have also been reported using intracellular techniques in neuronal microcircuits [1,34]. This search has recently seen significant progress [11,13,22] focusing on adaptation and plasticity at the network level but without investigating possible direct interactions of the delivered stimulus patterns. The paired-pulse protocols presented here can constitute a starting point for a more detailed interpretation of the observed plastic phenomena. Network plasticity could be sustained by a spike timing based mechanism taking place at specific temporal scales outside the observed suppression window. The complex stimulating protocols to interfere with the network's pathways can be considered as an extension of the single- and two-site protocols presented here.

Additionally, in the context of neural coding and bidirectional interfaces, our work suggest that at the network level there are extended refractory periods that should be taken into account. The faculty of a network to process and transmit incoming sensory information rely also on the ability to reconstruct time-varying input stimuli from the evoked responses [35]. The presented findings suggest the need for distributed stimuli and point out a possible role of an integrating window at short time scales ($<50$ ms). These preliminary insights based on the interactions between pulse responses, provide a first quantification of the way multiple stimuli contribute to the overall network response.

## ACKNOWLEDGMENTS

This work was partly supported by EU Contract No. 19247 Neurovers-IT. We thank Brunella Tedesco for the preparation of excellent cultures. We thank Thierry Nieus for critically reading the paper.

[1] G. G. Turrigiano and S. B. Nelson, Nat. Rev. Neurosci. **5**, 97 (2004).
[2] G. Q. Bi and M.-m. Poo, Annu. Rev. Neurosci. **24**, 139 (2001).
[3] S. Marom and G. Shahaf, Q. Rev. Biophys. **35**, 63 (2002).
[4] J. Malmivuo and R. Plonsey, *Bioelectromagnetism: Principles and Applications of Bioelectric and Biomagnetic Fields* (Oxford University Press, New York, 1995).
[5] R. S. Zucker and W. G. Regehr, Annu. Rev. Physiol. **64**, 355 (2002).
[6] C. C. McIntyre and W. M. Grill, Biophys. J. **76**, 878 (1999).
[7] J. B. Ranck, Jr., Brain Res. **98**, 417 (1975).
[8] D. A. Wagenaar, J. Pine, and S. M. Potter, J. Neurosci. Methods **138**, 27 (2004).
[9] Y. Jimbo, T. Tateno, and H. P. C. Robinson, Biophys. J. **76**, 670 (1999).
[10] G. Shahaf and S. Marom, J. Neurosci. **21**, 8782 (2001).
[11] M. Chiappalone, P. Massobrio, and S. Martinoia, Eur. J. Neurosci. **28**, 221 (2008).
[12] D. A. Wagenaar, J. Pine, and S. M. Potter, J. Negat. Results Biomed. **5**:16 (2006).
[13] R. Madhavan, Z. C. Chao, and S. M. Potter, Phys. Biol. **4**, 181 (2007).
[14] M. E. Ruaro, P. Bonifazi, and V. Torre, IEEE Trans. Biomed. Eng. **52**, 371 (2005).
[15] Y. Jimbo, A. Kawana, P. Parodi *et al.*, Biol. Cybern. **83**, 1 (2000).
[16] M. Chiappalone, A. Vato, L. Berdondini *et al.*, Int. J. Neural Syst. **17**, 87 (2007).
[17] D. A. Wagenaar, R. Madhaven, J. Pine *et al.*, J. Neurosci. **25**, 680 (2005).
[18] P. Darbon, L. Scicluna, A. Tscherter *et al.*, Eur. J. Neurosci. **15**, 671 (2002).
[19] E. Maeda, H. P. C. Robinson, and A. Kawana, J. Neurosci. **15**,

6834 (1995).
[20] D. Eytan, N. Brenner, and S. Marom, J. Neurosci. **23**, 9349 (2003).
[21] D. J. Bakkum, A. C. Shkolnik, G. Ben-Ary, P. Gamblen, T. B. Demarse, and S. Potter, *Embodied Artificial Intelligence*, edited by F. Iida, L. Steels, and R. Pfeiffer, Lecture Notes in Computer Science Vol. 3139 (Springer-Verlag, Berlin, 2004), p. 130–145.
[22] D. J. Bakkum, Z. C. Chao, and S. M. Potter, J. Neural Eng. **5**, 310 (2008).
[23] G. J. Brewer, J. R. Torricelli, E. K. Evege *et al.*, J. Neurosci. Res. **35**, 567 (1993).
[24] M. Chiappalone, M. Bove, A. Vato *et al.*, Brain Res. **1093**, 41 (2006).
[25] D. A. Wagenaar, J. Pine, and S. M. Potter, BMC Neurosci. **7**:11 (2006).
[26] P. Massobrio, G. Massobrio, and S. Martinoia, Neurocomputing **70**, 2467 (2007).
[27] A. Maccione, M. Gandolfo, P. Massobrio *et al.*, J. Neurosci. Methods **177**, 241 (2009).
[28] M. S. Lewicki, Network Comput. Neural Syst. **9**, R53 (1998).
[29] P. Bonifazi, M. E. Ruaro, and V. Torre, Eur. J. Neurosci. **22**, 2953 (2005).
[30] D. J. Bakkum, Z. C. Chao, and S. M. Potter, PLoS ONE **3**, e2088 (2008).
[31] W. H. Press, S. A. Teukolsky, W. T. Vetterling *et al.*, *Numerical Recipes in C++: The Art of Scientific Computing* (Cambridge University Press, Cambridge, England, 2002).
[32] I. Vajda, J. van Pelt, P. S. Wolters *et al.*, Biophys. J. **94**, 5028 (2008).
[33] J. Stegenga, J. le Feber, E. Marani *et al.*, IEEE Trans. Biomed. Eng. **56**, 1220 (2009).
[34] G. Q. Bi and M. M. Poo, Nature (London) **401**, 792 (1999).
[35] L. Cozzi, P. D'Angelo, and V. Sanguineti, Biol. Cybern. **94**, 335 (2006).